

Dependence of Striped Domain Growth on Background Wavenumber

Carina Kamaga, Denis Funfschilling, and Michael Dennin

Department of Physics and Astronomy, University of California at Irvine, Irvine, California 92697-4575

(Dated: November 23, 2018)

We report on the growth of domains of standing waves in electroconvection in a nematic liquid crystal. An ac voltage is applied to the system, forming an initial state that consists of travelling striped patterns with two different wavenumbers, zig and zag rolls. The standing waves are generated by suddenly applying a periodic modulation of the amplitude of the applied voltage that is approximately resonant with the travelling frequency of the pattern. By varying the modulation frequency, we are able to vary the steady-state, average wavenumber. We characterize the growth by measuring the structure factor for the pattern, the amplitude of the pattern, and the domain-wall length. An interesting feature of the growth is that the evolution of the domain-wall length is strongly affected by changing the selected wavenumber; whereas, the evolution of the structure factor is less sensitive to such changes.

PACS numbers: 47.54.+r,64.60.Cn

I. INTRODUCTION

When a system experiences a sufficiently large, sudden change of an external parameter, referred to as a quench, the current state of the system will lose stability and a transition will occur to a new state. When there is more than one possibility for the new state (such as spin up or down in a magnetic system), domains will form. At late times, these domains coarsen, or grow. The dynamics of this coarsening process has been the subject of substantial research and is important in many applications [1]. In general, the domains are characterized by a single length scale, $l(t)$, that grows according to a power-law, $l(t) \sim t^n$. Here n is referred to as the *growth exponent*. This process is usually referred to as *domain coarsening*. Some examples of systems for which domain coarsening has been studied in detail [1], either theoretically or experimentally, include the Ising model, binary fluids, liquid crystals, diblock copolymers [2, 3], and electroconvection [4].

There are a number of ways to categorize systems undergoing coarsening. First, one must distinguish between cases where the order parameter is conserved, such as in a binary fluid, and where it is not conserved, such as in the Ising model. Second, the domains that are growing may be uniform, such as in both the Ising model and binary fluids, or they may consist of a pattern, such as stripes in the case of diblock copolymers and electroconvection. Finally, the initial and final states can either be thermodynamic equilibrium states or steady states of the system. Most of the studies have focused on the case where the initial state prior to the quench and the final state well after the quench are thermodynamic equilibrium states [1]. We will refer to this type of system as a *thermodynamic system*. For isotropic, thermodynamic systems, where the domains are uniform, the exponents are well known. For systems with a non-conserved order parameter, $n = 1/2$. Systems with a conserved order parameter have $n = 1/3$. In this report, we focus on coarsening in a system in which the domains are composed of stripes.

An added feature of the system we consider is that the initial and final states are *not* states of thermodynamic equilibrium, though they are steady-states of the system. We refer to this as a driven system.

For systems in which the domains are composed of stripes, theoretical studies of the power-law scaling of the late-time domain growth has focused on simulations and analysis of the Swift-Hohenberg equation [5, 6, 7, 8, 9, 10, 11]. Experiments have been performed in both a thermodynamic system, diblock copolymers [2, 3], and a driven system, electroconvection [4, 12]. This work has raised two related issues. First, two length scales are important in the problem: the wavelength of the pattern and the scale of a domain. This has an interesting impact on the measured growth exponents. Traditional studies of domain growth focus on the structure factor, $S(k)$. This measures both variations in wavenumber and domain size, with information about both lengths scales mixing in a nontrivial way. For striped systems, one can also consider orientational correlation functions, defect densities, or domain wall lengths. These quantities are independent of the local wavenumber and are expected to provide information about domain size only.

Numerical simulations have considered both the scaling of the structure factor, $S(k)$, of the system and the orientational correlation function. The evolution of the structure factor is found to be consistent with a length scale that grows as $t^{1/5}$ for both potential and nonpotential versions of the Swift-Hohenberg equation [6, 7]. However, the growth exponent determined from the orientational correlation function is $1/4$ for the potential case and $1/2$ for the nonpotential case [6]. The orientational correlation function and defect densities are measured experimentally in diblock copolymers [2]. The results agree with the potential case of the Swift-Hohenberg model, $n = 1/4$. For a particular case of electroconvection, it was shown that the wavenumber and domains evolve differently [4]. It was found that the growth exponent measured using $S(k)$ is consistent with $n = 1/5$ and measurement of the domain size gave $n = 1/4$. This is

in agreement with simulations for the potential case [6]. In addition, the distribution of local wavenumbers was measured separately. This distribution was essentially independent of time, providing an explanation for the difference between $S(k)$ and domain wall measurements.

The second issue associated with striped domains is the interaction between defects in the pattern and the background stripe pattern. This has been studied using the Swift-Hohenberg equation. One important consequence is that the growth of domains can be strongly affected by pinning of grain boundaries [8, 9]. In these simulations, the measured growth exponents depends on the depth of the quench, something that does not occur in uniform systems. The growth exponents are also found to depend on the level of noise in the system [5, 10]. This is attributed to the fact that noise can provide a source of “depinning” for the defects. Finally, the evolution of the average wavenumber provides a possible explanation for differences in simulations of the potential and nonpotential versions of the Swift-Hohenberg equations. The average wavenumber in each case evolves to different values, and this was suggested as one possible explanation for the two different growth exponents [6].

We report on an experimental study of the impact of changes in the average wavenumber on the growth of domains. We utilize a particular example of electroconvection that is ideally suited for controlling the average wavenumber of the pattern: electroconvection in the nematic liquid crystal I52 [13, 14]. A nematic liquid crystal is a fluid in which the molecules are aligned on average [15]. The axis along which the average alignment points is referred to as the director. For electroconvection [16], a nematic liquid crystal is placed between two glass plates that have been treated so that the director is everywhere parallel to the plates. An ac voltage is applied perpendicular to the plates. Above a critical value of the voltage, a pattern of stripes forms. Because the system is anisotropic (the director selects a preferred axis), the states are usually characterized by the angle between the wavevector of the pattern and the undistorted director, θ . States with the same wavenumber and angle $\pm\theta$ are degenerate and referred to as zig and zag, respectively. For the system discussed in this paper, the initial pattern consists of four travelling stripe states [17]: right- and left-travelling zig and zag rolls. It has been established for this system that above a critical value for a modulation of the applied voltage at twice the travelling frequency, the system consists of either standing zig or zag rolls [14]. Therefore, a sudden quench of the system from below this critical value to above it results in the nucleation of domains of standing zig and zag rolls, which proceed to coarsen.

Previous measurements of growth exponents for this system focused on quenches that used exactly twice the travelling frequency. Reference [4] reports a value of $n = 1/4$ for the growth of the domain size and $n = 1/5$ for the scaling of $S(k)$. A single initial experiment for a modulation frequency slightly different from twice the trav-

elling frequency suggested similar behavior. However, a systematic exploration of changes in the wavenumber, by varying the modulation frequency, is possible for this system [14], and has not been carried out. In this paper, we report on such a study. The rest of the paper is organized as follows. Section II provides the details of the experimental system and the techniques used to analyze the domain growth. Section III presents the results of the experiment. Section IV provides a discussion of the results.

II. EXPERIMENTAL DETAILS

We used the liquid crystal I52 [18] doped with iodine. Due to the nature of I52, 8% iodine by weight was used initially. However, a significant fraction of the iodine evaporates before the cells are filled, so the final concentration is not well controlled. We used commercial liquid crystal cells [19] composed of two transparent glass plates coated with a transparent conductor, indium-tin oxide. The cells were 2.54 cm x 2.54 cm, with the conductor forming a square 1 cm x 1 cm in the center of the cell. The glass was also treated with a rubbed polymer to obtain uniform planar alignment of the director. We define the direction parallel to the undistorted director to be the x axis and the direction perpendicular to the undistorted director to be the y axis.

The apparatus is described in detail in Ref. [20]. It consists of an aluminum block with glass windows. The temperature of the block was kept constant to ± 0.001 °C. Polarized light is applied from the bottom of the cell. Above the cell, there is a ccd camera to capture the image of patterns using the standard shadowgraph technique [21].

We apply an ac voltage of the form $V(t) = \sqrt{2}[V_o + V_m \cos(\omega_m t)] \cos(\omega_d t)$ perpendicular to the glass plates. Here V_o is the amplitude of the applied voltage in the absence of modulation, V_m is the modulation amplitude, ω_m is the modulation frequency, and ω_d is the driving frequency. For all of the experiments reported on here, $\omega_d/2\pi = 25$ Hz. The critical voltage, V_c is defined as the value of V_o for which the system makes a transition from a uniform state to the superposition of travelling rolls *in the absence of modulation*. There are two relevant control parameters: $\epsilon = (V_o/V_c)^2 - 1$ and $b = V_m/V_c$.

For the experiments discussed here, the system is initially at $\epsilon = 0.04$ and $b = 0$, i.e. above onset with no modulation. As mentioned in Sec. I, there are only four modes needed to describe the observed convection rolls: zig and zag, right and left travelling oblique rolls. This state is an example of spatiotemporal chaos in that the amplitude of the four modes varies irregularly in space and time [22]. For each ϵ and ω_m , there exists a critical value of b , b_c , above which the system consists of standing zig and zag rolls. A quench corresponds to a sudden change of b to some value $b > b_c$. At and below V_c , the modulation frequency with the strongest coupling

to the pattern, and correspondingly smallest value of b_c , is twice the Hopf frequency, ω_h . The Hopf frequency is the travelling wave frequency at V_c . As one increases ϵ , the natural frequency of the pattern shifts. Because we worked at a finite value of ϵ , the smallest value of b_c occurs for a modulation frequency, $\omega_m = 2\omega^*$, where ω^* is the natural frequency of the pattern at the given value of ϵ . Because it is the relative shift in frequency that matters, we will consider the behavior as a function of $\delta f = f^* - f_m/2$, where $f^* = \omega^*/2\pi$ and $f_m = \omega_m/2\pi$. Figure 1 is a plot of b_c as a function of δf for $\epsilon = 0.04$. We focus almost exclusively on the negative values of δf because for $\delta f > +0.01$ Hz, the pattern stabilized by modulation is standing waves that are a superposition of zig and zag rolls, and not individual domains of standing zig and zag rolls.

Quenches were performed for a range of δf . The final value of b in each case was selected so that the quench depths all corresponded to $\Delta b = 0.02$, as measured from the onset of standing waves (solid curve in Fig. 1). The camera was triggered to take the images at the same point in the modulation cycle. This ensured that the pattern was imaged at the same point in the standing wave cycle. Each image covered a region of $4.1 \text{ mm} \times 3.1 \text{ mm}$ of the cell. Time is scaled by the director relaxation time, $\tau_d \equiv \gamma_1 d^2 / (\pi^2 K_{11}) = 0.2 \text{ s}$. Here γ_1 is a rotational viscosity; K_{11} is the splay elastic constant; and d is the thickness of the cell.

An example of a small region of the pattern after a quench is given in Fig. 2. Two different quenches are illustrated: $\delta f = 0.008 \text{ Hz}$ and $\delta f = -0.23 \text{ Hz}$. The images for $\delta f = 0.008 \text{ Hz}$ illustrate the type of patterns on which we focused: standing zig and zag rolls separated by domain walls. The domain walls are relatively “thick”, and the superposition of zig and zag rolls in a domain wall is visible. The quench at $\delta f = -0.23 \text{ Hz}$ illustrates qualitatively different behavior. In this case, there are regions of superposition that are “domains” in their own right, though most of the regions of superposition can be considered to be domain walls. As we will show, this qualitative difference is apparent in various characterizations of the growth. As the focus of the paper is the impact of varying the wavenumber on the domain growth in the zig/zag system, we will only report on this single quench in the regime where domains of the superposition of zig and zag rolls occurs. Further increasing $|\delta f|$ results in patterns that are entirely the superposition of zig and zag rolls. Future work will consider in more detail this other class of patterns.

A number of features of the domains were analyzed. First, the power spectrum, $S(k)$, of each image was computed. This was used to determine the average wavenumber ($\langle k \rangle \equiv \int k S(k) dk / \int S(k) dk$) for the zig and zag rolls. The widths of the fundamental peak in $S(k)$ in both the x (σ_x) and y (σ_y) directions were determined using the second moment of $S(k)$. This gives $\sigma_x \equiv \sqrt{\langle k_x^2 \rangle - \langle k_x \rangle^2}$, with $\langle k_x^2 \rangle \equiv \int k_x^2 S(k) dk / \int S(k) dk$, and a similar definition for σ_y .

(Note: all of the integrals were taken as sums over a finite region around the fundamental peak, as described in Ref. [4].) σ_x and σ_y contain information about the typical size of a domain and the distribution of wavenumbers, in the respective directions.

We also analyzed the images by first converting them to a scaled image of zig and zag domains, referred to as the *angle map*. This was done using the procedure detailed in Ref. [4]. Briefly, the local angle of the wavenumber is computed using the algorithm reported in Ref. [23]. This is used to produce an image with black and white domains representing regions of zig and zag, respectively. Regions of superposition of zig and zag rolls (the domains wall for most of the quenches) are represented by gray. Figure 3 illustrates a typical image (Fig. 3a) and the results after conversion to an angle map (Fig. 3b). Once these images are produced, two measures of the domain growth that are independent of variations in the local wavenumber are computed. First, one can determine the total domain wall length per viewing area, L . This quantity scales as the inverse of a characteristic domain size (the area of the viewing scales as a length squared). In our case, L was defined as the total number of gray pixels divided by the total area of the image. For all of the quenches except the ones at $\delta f = -0.23 \text{ Hz}$, the width of the domain walls was constant during the domain growth. Therefore, this is a consistent measure of the total domain wall length. For the quench at $\delta f = -0.23 \text{ Hz}$, we still used this definition for consistency, even though it represents a transitional behavior. In this case, some of the regions of superposition of zig and zag rolls (gray pixels) are more appropriately considered domains in their own right. Still, most of the gray pixels corresponded to domain walls between zig and zag domains. We also computed the power spectrum of the angle map image, $S(q)$. In this case, the peak is centered at $q = 0$, as the angle map domains are uniform. Therefore, the width of the peak is related to the typical domain size only. Again, we separately considered the width in the x direction (w_x) and y direction (w_y), where the widths are defined in the same manner as for $S(k)$.

III. RESULTS

Figure 4 shows the time evolution of the average wavenumber ($\langle k \rangle$) for the different quenches of interest. A number of features of the evolution are evident. First, as claimed, the steady-state value of the $\langle k \rangle$ is dependent on δf (see Fig. 4a). However, for all quenches, the $\langle k \rangle$ is still evolving even at late times. After $t/\tau_d \approx 1000$, the evolution is consistent with a very slow logarithmic growth: $\langle k \rangle = a \log_{10}(t/\tau_d)$, with $a \approx 0.01$. This is illustrated in Fig. 4b. However, for all but the largest value of $|\delta f|$, there is a weak dependence on when the logarithmic growth begins (with values ranging from $2.7 < \log_{10}(t/\tau_d) < 3.1$) and on the coefficient (a) of the logarithmic growth (with values ranging from 0.006

to 0.02. In general, for larger $|\delta f|$, evolution consistent with logarithmic time dependence occurs at a later time. As referred to in Sec. II, for $\delta f = -0.23$ Hz, the pattern is qualitatively different. In this case, the evolution of $\langle k \rangle$ is also very different, with logarithmic growth setting in significantly later ($\log_{10}(t/\tau_d) \approx 3.5$) and with a coefficient of 0.05.

Figure 5 shows the evolution of the width of the power spectrum for both the pattern (σ_x and σ_y) and the angle map (w_x and w_y). There are a number of features that become apparent in these plots. First, if one were to assume that a scaling regime is reached, the growth exponent measured from $S(k)$ is very different from that measured for $S(q)$. Based on σ_x and σ_y , one observes very slow growth for the system. For late times, assuming $\sigma \sim t^n$, the exponents n are on the order of 0.1. In contrast, the length scales characterized by the inverse of w_x and w_y grow faster. In this case, one obtains growth exponents of $n = 0.33$ or larger. This difference is consistent with earlier results comparing $S(k)$, which includes information about the variation in local wavenumber, to more direct measures of the domain size [4, 6].

The second feature of the growth is the differences between the growth in the x- and y-directions. For the quench with $\delta f = 0.008$ Hz, both w_x and w_y have the same magnitude and time dependence. This suggests that the system is evolving in a relatively isotropic manner. For σ_x and σ_y , the time evolution is similar, though the magnitudes are different. This suggests that there is more anisotropy in the local wavenumber distributions than there is in the domains. This anisotropy contributes to the difference in magnitude between σ_x and σ_y , but does not impact the time evolution. For the case of $\delta f = -0.23$ Hz, the situation is roughly reversed. In this case, σ_x and σ_y have roughly the same magnitude throughout the evolution. In contrast, w_x and w_y have different magnitudes and slightly different time evolution, at late times. This qualitative difference is probably due to the increased area of the pattern that is given by a superposition of zig and zag rolls, and thus, the change in the nature of the domain boundaries.

As an alternative measure of the domain growth, we also considered the total domain wall length present in a fixed viewing area. This measure is an *isotropic* measure of the domain growth. Its time evolution is a good measure of how rapidly the overall size of a domain changes. However, it does not provide any information about the relative rate of change in the x- and y-direction. Figure 6 shows the evolution of the total domain wall length for a number of values of δf . Also shown are two straight lines that provide a guide to the eye. The dashed line has a slope of -0.7 , and the solid line has a slope of -0.3 . It is clear from this plot that the evolution of the domain size occurs more rapidly for the larger values of $|\delta f|$.

At this point, it is important to emphasize one of the challenges of interpreting data used to characterize domain growth. In studies of domain coarsening, it is standard to assume that a late-time scaling regime ex-

ists in which the lengths characterizing the domain size grow as a power-law in time. One experimental difficulty with this assumption is determining when such a scaling regime is reached. This is especially true in the studies reported on here, where the average wavenumber is still evolving in time for all of the conditions that we studied (even if it is only logarithmic in time). However, independent of whether or not a true scaling regime has been reached, for similar times during the evolution of the domains, the data is consistent with a power-law of the form $l(t) \sim t^n$, where l is some characteristic length. Therefore, the values of n provide information about the relative rate of growth of domains under different circumstances. This is our main motivation for looking at n . Any claims of a true scaling regime would be premature at this point, though the consistency of the data with power-law behavior suggests that it is possible such a regime has been reached.

Figure 7 summarizes the impact of variations in the wavenumber on the domain growth by comparing growth exponents n for w_x , w_y , and the total domain wall length per viewing area L . The results from σ_x and σ_y exhibited no strong dependence on δf . One observes that the growth of the domains is significantly faster for larger $|\delta f|$, as measured by the total domain wall length in a given area. In this case, n increases in magnitude monotonically with $|\delta f|$. However, the trends in w_x and w_y are less obvious. If anything, one observes a small change in the magnitude of n for w_x and w_y as $|\delta f|$ is increased. Also, the growth appears to become more anisotropic as $|\delta f|$ increases.

IV. SUMMARY

The experiments reported on here demonstrate the close connection between the dynamics of domain growth in patterned systems and the evolution of the background wavenumber. We performed a series of quenches in which the steady-state average wavenumber after the quench is varied. The resulting domain growth depends on the evolution and steady-state value of $\langle k \rangle$. However, different measures of the domain growth are impacted to different degrees. A direct measure of the typical domain size, the average domain wall length in a fixed viewing area, showed the strongest dependence on the average wavenumber, with the rate of growth increasing as the wavenumber is varied away from its “natural” value.

If one assumes that the average domain wall length scales as a power in time, exponents in the range of 0.3 to 0.7 are observed. As discussed in the introduction, such a large variation in growth exponent is consistent with simulations of the two different Swift-Hohenberg equations [6]. In Ref. [6], the calculated exponent is found to increase from 0.25 to 0.5 with a variation in wavenumber of approximately 20%. This difference in average wavenumber was suggested as the source of the different exponents. The work in Ref. [6] does not directly

apply to this system because it considered the isotropic Swift-Hohenberg equation, and our system is anisotropic. However, the similarity between the two results suggests that it is worth further work to determine how universal the impact of wavenumber variation is on domain growth in patterned systems.

An interesting feature of the growth is that as one forced the average wavenumber to be different from the “natural” wavenumber of the system, the rate of growth was increased. In our case, the maximum variation in wavenumber was only 6%, but the exponent changed from 0.3 to 0.7. If these results carry over to other patterned systems, such as diblock copolymers, one can have a relatively significant impact on the rate of growth of

domains by inducing a change in the average wavenumber away from the “natural” wavenumber. This increase in the rate of domain coarsening could have a practical impact in various processing situations.

Acknowledgments

This work was supported by NSF grant DMR-9975479. M. Dennin also thanks the Research Corporation and Alfred P. Sloan Foundation for additional funding for this work.

-
- [1] A. J. Bray, *Advances in Physics* **43**, 357 (1994).
 - [2] C. Harrison, D. H. Adamson, Z. Cheng, J. Sebastian, S. Sethuraman, D. Huse, R. A. Register, and P. M. Chaikin, *Science* **290**, 1558 (2000).
 - [3] C. Harrison, Z. Cheng, S. Sethuraman, D. A. Huse, P. M. Chaikin, D. A. Vega, J. M. Sebastian, R. A. Register, and D. H. Adamson, *Phys. Rev. E* **66**, 011706 (2002).
 - [4] L. Purvis and M. Dennin, *Phys. Rev. Lett.* **86**, 5898 (2001).
 - [5] K. R. Elder, J. Vinals, and M. Grant, *Phys. Rev. Lett.* **68**, 3024 (1992).
 - [6] M. C. Cross and D. I. Meiron, *Phys. Rev. Lett.* **75**, 2152 (1995).
 - [7] J. J. Christensen and A. J. Bray, *Phys. Rev. E* **58**, 5364 (1998).
 - [8] D. Boyer and J. Vinals, *Phys. Rev. E* **64**, 050101 (2001).
 - [9] D. Boyer and J. Vinals, *Phys. Rev. E* **65**, 046119 (2002).
 - [10] T. Taneike, T. Nihei, and Y. Shiwe, *Phys. Lett. A* **303**, 212 (2002).
 - [11] H. Qian and F. Mazenko, arXiv:cond-mat/0210334 (2002).
 - [12] C. Kamaga, F. Ibrahim, and M. Dennin, preprint (2003).
 - [13] M. Dennin, D. S. Cannell, and G. Ahlers, *Phys. Rev. E* **57**, 638 (1998).
 - [14] M. Dennin, *Phys. Rev. E* **62**, 7842 (2000).
 - [15] P. G. de Gennes and J. Prost, *The Physics of Liquid Crystals* (Clarendon Press, Oxford, 1993).
 - [16] L. Kramer and W. Pesch, *Annu. Rev. Fluid Mech.* **27**, 515 (1995).
 - [17] M. Dennin, M. Treiber, L. Kramer, G. Ahlers, and D. S. Cannell, *Phys. Rev. Lett.* **76**, 319 (1996).
 - [18] U. Finkenzeller, T. Geelhaar, G. Weber, and L. Pohl, *Liq. Cryst.* **5**, 313 (1989).
 - [19] E.H.C. CO., Ltd., 1164 Hino, Hino-shi, Tokyo, Japan.
 - [20] M. Dennin, *Phys. Rev. E* **62**, 6780 (2000).
 - [21] S. Rasenat, G. H. B. L. Winkler, and I. Rehberg, *Experiments in Fluids* **7**, 412 (1989).
 - [22] M. Dennin, D. S. Cannell, and G. Ahlers, *Science* **272**, 388 (1996).
 - [23] D. A. Egolf, I. V. Melnikov, and E. Bodenschatz, *Phys. Rev. Lett.* **80**, 3228 (1998).

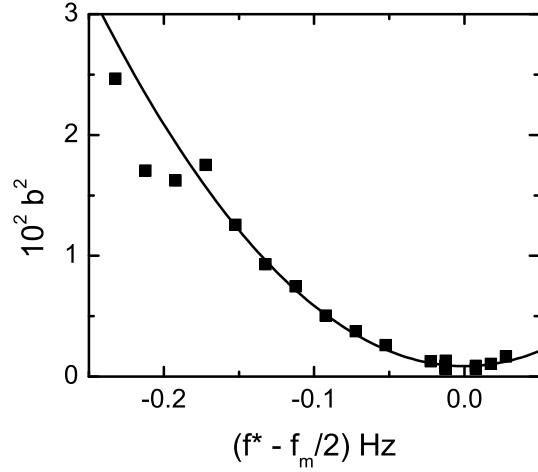


FIG. 1: Onset curve for standing waves at a value of $\epsilon = 0.04$ as a function of $\delta f = f^* - f_m/2$. Here f^* is the natural travel frequency of the pattern at $\epsilon = 0.04$ and f_m is the modulation frequency. The parameter $b = V_m/V_c$, where V_m is the modulation voltage and V_c is the critical voltage for the onset of a pattern in the absence of any modulation. The solid line is a fit to the data used to determine f^* .

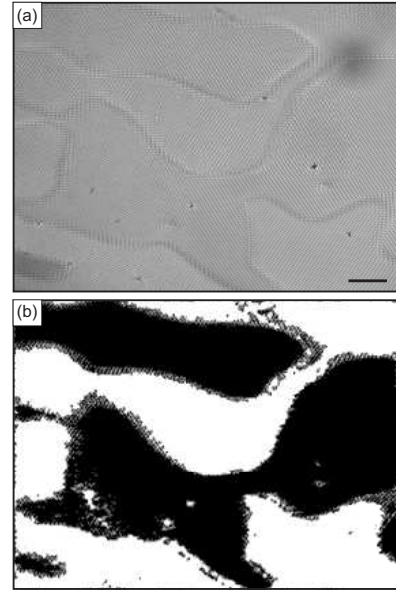


FIG. 3: (a) Image taken 384 s after a quench with $\delta f = 0.008$ Hz. (b) The same image converted to an “angle” map. The black and white regions are zig and zag rolls, respectively. The gray regions are the boundaries between domains. The scale bar in (a) represents 0.4 mm.

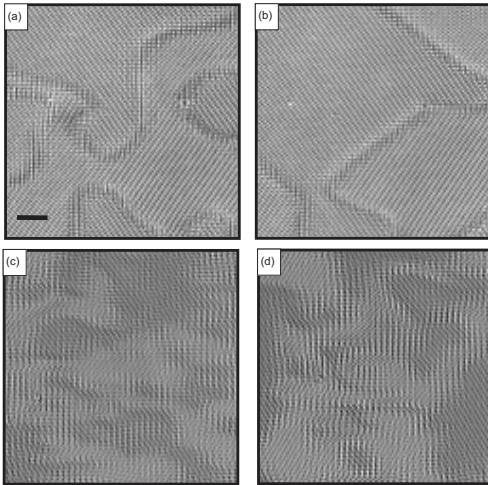


FIG. 2: Four images of domain growth. Images (a) and (b) are with a modulation frequency $\delta f = 0.008$ Hz, at $t = 96$ s and $t = 600$ s after the quench, respectively. Images (c) and (d) are with a modulation frequency $\delta f = -0.23$ Hz, at $t = 107$ s and $t = 667$ s after the quench, respectively. The solid bar in (a) is 0.2 mm.

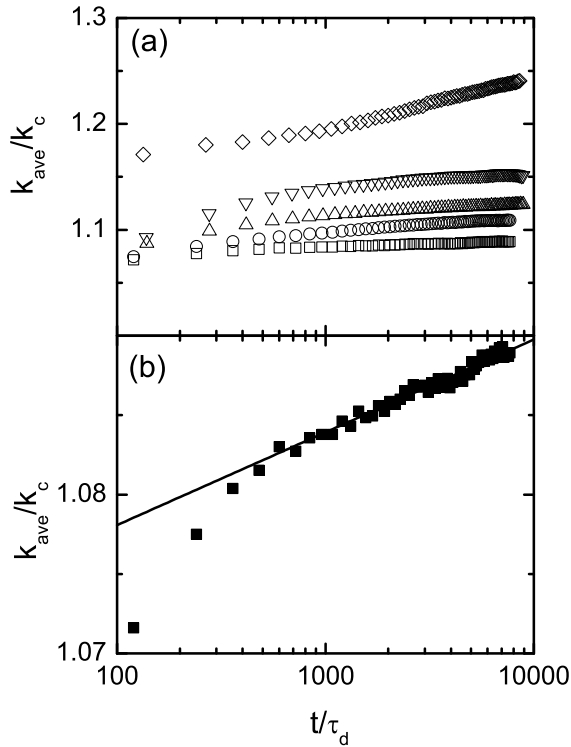


FIG. 4: (a) Average wavenumber for the zig standing rolls as a function of time after the quench. Time is scaled by the director relaxation time, τ_d . The symbols are as follows: (\square) $\delta f = 0.008$ Hz, (\circ) $\delta f = -0.012$ Hz, (\triangle) $\delta f = -0.022$ Hz, (∇) $\delta f = -0.072$ Hz, and (\diamond) $\delta f = -0.23$ Hz. The wavenumber for the zag rolls shows similar behavior. (b) An expanded view of the average wavenumber for $\delta f = 0.008$ Hz. The solid line is a guide to the eye illustrating the regime where the evolution of $\langle k \rangle$ is consistent with logarithmic growth in time.

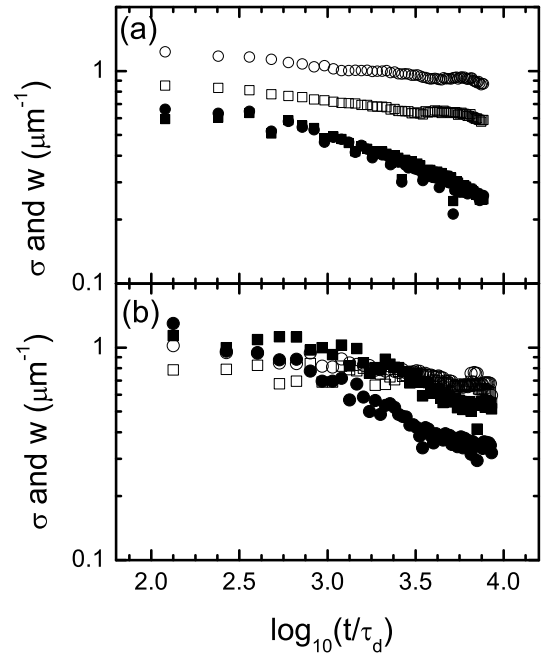


FIG. 5: Width of the power spectrum as a function of time for two different values of δf . Time is scaled by the director relaxation time τ_d . (a) $\delta f = 0.008$ Hz (b) $\delta f = -0.23$ Hz. In both cases, the open symbols are for the power spectrum computed on the image with the stripes, with σ_x given by the squares and σ_y given by the circles. The closed symbols are for the power spectrum of the image of the angle map, with w_x given by the squares and w_y given by the circles.

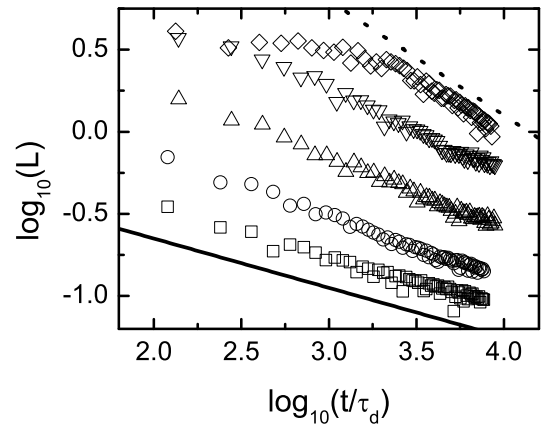


FIG. 6: Total domain wall length as a function of time for all the quenches studied. Time is scaled by the director relaxation time, τ_d . The symbols are as follows: (\square) $\delta f = 0.008$ Hz, (\circ) $\delta f = -0.012$ Hz, (\triangle) $\delta f = -0.022$ Hz, (∇) $\delta f = -0.072$ Hz, and (\diamond) $\delta f = -0.23$ Hz. The lines are provided as a guide to the eye, with the dashed line having a slope of -0.7 and the solid line having a slope of -0.3 .

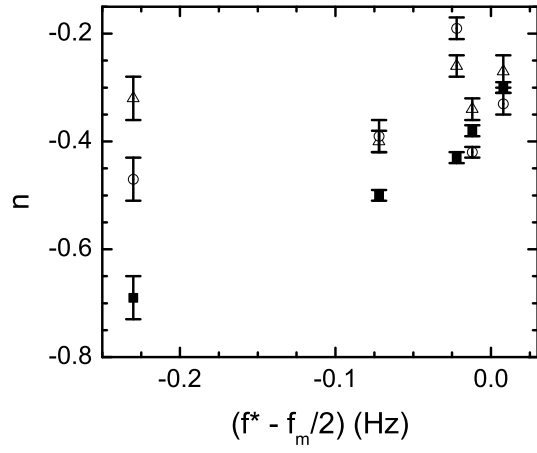


FIG. 7: Summary of measured scaling exponents (n) for both the domain wall length (solid squares), w_x (open triangles), and w_y (open circles).